K. C. Gupta
Associate Professor,
Department of Materials Engineering,
University of Illinois
at Chicago Circle,
Chicago, Ill. 60680
Mem. ASME

B. Roth
Professor,
Department of Mechanical Engineering,
Stanford University,
Stanford, Calif. 94305

Design Considerations for Manipulator Workspace

This paper introduces some basic concepts regarding the workspaces of manipulators. The first part gives a general discussion regarding workspace shapes. Most of the rest of the paper focuses on manipulators with three orthogonal mutually intersecting axes. The structures of the primary and secondary workspaces for such systems are determined and the effects of hand size are examined in detail. Several specific examples are presented to illustrate the basic theory.

Introduction

There has been much interest in the kinematic design of manipulators. One of the basic questions is determining the shape of the workspace [1–5]. There are two issues: Given the structure, what is the workspace? Alternatively, given a desired workspace, what should the manipulator's structure be? This paper treats both of these questions and endeavors thereby to expand our understanding of these complex devices.

Workspace of a Point

One way of defining the workspace of a manipulator is as the aggregate of all possible positions of a point attached to the free end of the manipulator. This point is usually located at either the center of the "wrist," the center of the "hand," or the tip of a "finger."

Consider the system shown in Fig. 1 where the manipulator has n-degrees of freedom by virtue of n revolute joints in series. The first link is attached to a fixed frame and the $(n+1)^{th}$ link contains the reference point P. The axes of the joints are labeled in numerically ascending order.

The workspace of point P is the aggregate of all points (in the fixed frame) which P occupies as the joint axes are rotated through their complete ranges. Let $W_k(P)$ denote the workspace of point P with respect to a frame fixed in the kth link. The workspace $W_{k-1}(P)$ is then obtained by revolving $W_k(P)$ about the $k-1$ axis.

The operation of revolving the workspace $W_{k+1}(P)$ about axis k can be represented by:

$$R_k[W_{k+1}(P)] = W_k(P).$$

Considering a sequence of such operations, starting from the axis closest to the free end, we have

$$W_n(P) = \text{circle}(n)$$

$$W_{n-1}(P) = R_{n-1}[W_n(P)] = R_{n-1}[\text{circle}(n)] = \text{torus}(n-1)$$

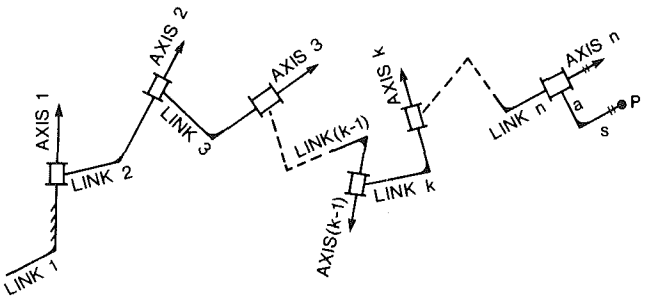

Fig. 1 A manipulator with n revolute axes in series and a point P attached to the free end

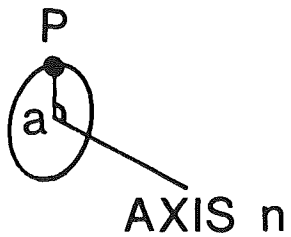

Fig. 2 Workspace $W_n(P)$ = circle (n)

$$W_{n-2}(P) = R_{n-2}[W_{n-1}(P)] = R_{n-2}[\text{torus}(n-1)] = \text{SHR}(n-2)$$

$$W_{n-3}(P) = R_{n-3}[W_{n-2}(P)] = R_{n-3}[\text{SHR}(n-2)] = \text{SHR}(n-3)$$

$$\vdots$$

$$W_1(P) = R_1[W_2(P)] = R_1[\text{SHR}(2)] = \text{SHR}(1)$$

By circle (n) we mean the circle generated by point P as it is rotated about axis n. The torus $(n-1)$ is the workspace of point P as it rotates about axes n and $n-1$; it is the surface generated by circle (n) as it is revolved about axis $(n-1)$. These are shown in Figs. 2 and 3.

Contributed by the Mechanisms Committee and presented at the Design Engineering Technical Conference, Hartford, Conn., September 20–23, 1981, of THE AMERICAN SOCIETY OF MECHANICAL ENGINEERS. Manuscript received at ASME Headquarters, June 11, 1981. Paper No. 81-DET-79.

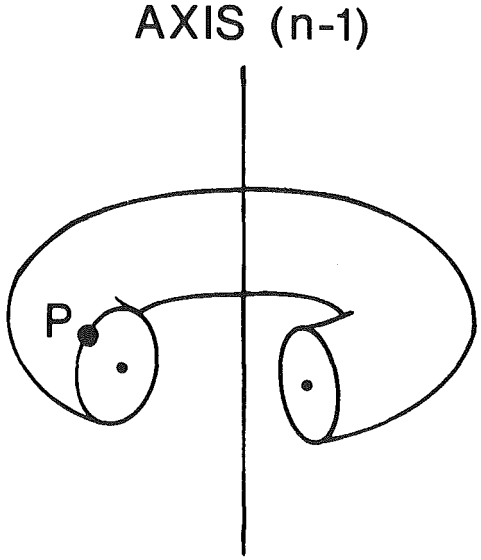

Fig. 3 Workspace $W_{n-1}(P)$ = torus $(n-1)$

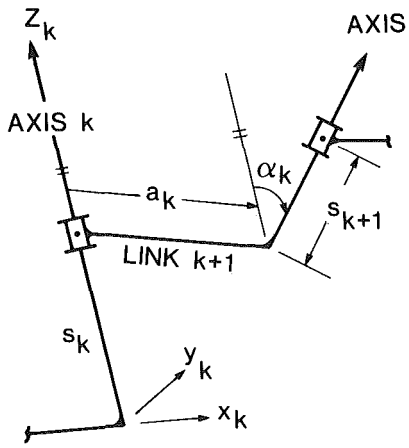

Fig. 4 Standard notation for link parameters. Shown are twist angle α_k, axial dimension s_{k+1}, and transverse dimension a_k of link $k+1$.

Using the standard nomenclature defined in Fig. 4, we can write the equation for the torus $(n-1)$ in the $x_{n-1}, y_{n-1}, z_{n-1}$ coordinate system:

$$[x_{n-1}^2+y_{n-1}^2+(z_{n-1}-s_{n-1})^2-(a_{n-1}^2+a^2+(s+s_n)^2)]^2$$
$$=4a_{n-1}^2\left[a^2-\left(\frac{(z_{n-1}-s_{n-1})-(s+s_n)\cos\alpha_{n-1}}{\sin\alpha_{n-1}}\right)^2\right] \quad (1)$$

a and s in equation (1) are as shown in Fig. 1. It is known that the torus may have a variety of shapes [6].

The degenerate forms which follow directly from (1) are

$a_{n-1}=0$, the real locus of P is a segment of a sphere
$\alpha_{n-1}=0$, the real locus of P is a segment of a plane
$a=0$, the real locus of P is a circle

The common anchor ring or right circular form of the torus is obtained when $\alpha_{n-1} = 90$ deg and $s_n = -s$. In this case, any plane containing the z_{n-1} axis cuts the torus into two circles.

For the flattened form $s_n = -s$, but $\alpha_{n-1} \neq 90$ deg; the section by a plane containing the z_{n-1} axis is now two egg-shaped curves—which, like the circles, are everywhere convex.

The symmetrical-offset form with $\alpha_{n-1} = 90$ deg, but $s_n \neq -s$ has various shapes. For $s_n \approx -s$ and $a < a_{n-1}$, the cross sections are similar to the circles of the right circular form.

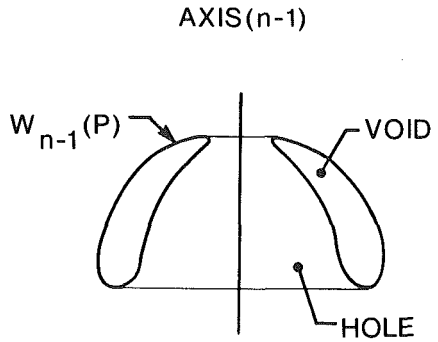

Fig. 5 Section of $W_{n-1}(P) \equiv$ torus $(n-1)$ by a plane containing axis $(n-1)$. Regions termed hole and void are shown.

However, as a approaches the length a_{n-1}, the inner walls become flatter. When $a > a_{n-1}$, the inner walls become concave and the section has two banana-shaped closed curves.

When we have a general form, the shape depends on a, a_{n-1}, s_n, s, and α_{n-1}. However, it is important to note that if $a/a_{n-1} << 1$, we have a hole surrounding the $n-1$ axis and the section will be as, for example, shown in Fig. 5. The hole is not always present; if a is large enough, the torus may intersect itself. This will occur whenever the axis $n-1$ passes through the inside or the circumference of circle (n). The analytical condition for this is

$$a^2 \geq a_{n-1}^2 + (s+s_n)^2\tan^2\alpha_{n-1} \quad (2)$$

It follows therefore that if $s + s_n$ or α_{n-1} are zero, there will not be a hole if $a \geq a_{n-1}$. On the other hand, if $\alpha_{n-1} = 90$ deg, there will always be a hole unless $s_n = -s$. Thus in the popular 90 deg case, the designer automatically introduces a hole unless $s_n = -s$. Equation (2) tells us that if $s_n \neq -s$, α_{n-1} should never be 90 deg if we want to avoid having a hole in the workspace $W_{n-1}(P)$.

Equation (2) provides a useful tool for determining the dimension a. Furthermore, it can be used recursively to determine the link lengths if we wish to size a system which folds back on itself so that each joint can reach the previous axis:

$$a_k^2 \geq a_{k-1}^2 + s_k^2\tan^2\alpha_{k-1},\ k=2,\ \ldots,n-1 \quad (3)$$

Here we use the equal sign if we wish to exactly reach, and the inequality if we wish to reach beyond, the previous axis.

We have used the abbreviation SHR for the *solid portion of a hollow ring*. The volume-of-revolution generated by revolving torus $(n-1)$ about axis $n-2$ can be such that it contains all the points within its boundaries or it can have empty spaces within it. There are two distinctly different types of empty spaces. The first we call a *hole*; it occurs whenever axis $n-2$ does not intersect torus $(n-1)$. (The transition condition for this follows if we set $x_{n-1} = -a_{n-2}$ and $y_{n-1} = z_{n-1}\cot\alpha_{n-2}$ in the equation for torus $(n-1)$ and find the condition for a double real root to exist.)

The other type of empty space occurs if α_{n-2} is large whenever torus $(n-1)$ has a hole, or the axis $(n-2)$ cuts the torus $(n-1)$, or the axes $n-1$ and $n-2$ are nearly the same. We call this space a *void* (internal hole). Figures 5 and 6 illustrate holes and voids in torus $(n-1)$ and SHR $(n-2)$.

From the foregoing, it follows that voids will not exist in SHR $(n-2)$ if the axis $(n-2)$ does not pass through the void of torus $(n-1)$, and α_{n-2} is small whenever torus $(n-1)$ has a hole, and the axes $n-1$ and $n-2$ are distinct. The critical value of α_{n-2} when torus $(n-1)$ has a hole is 90-β where β is the angle between the axis and bitangent of the torus $(n-1)$.

The generalizations to SHR (k) and SHR $(k-1)$ obtained from it are as follows: SHR $(k-1)$ has a hole whenever the axis $k-1$ does not cut SHR (k). SHR $(k-1)$ has a void if α_{k-1}

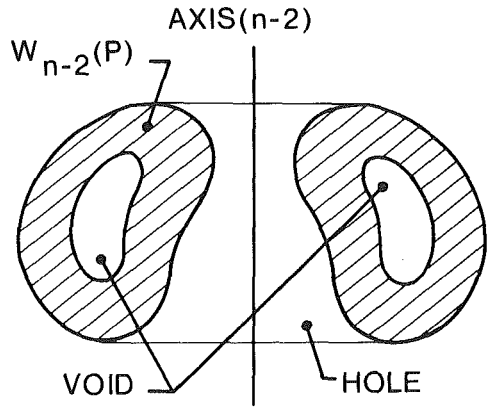

Fig. 6 Cross section of $W_{n-2}(P) \equiv$ SHR $(n-2)$ with hole and void labeled

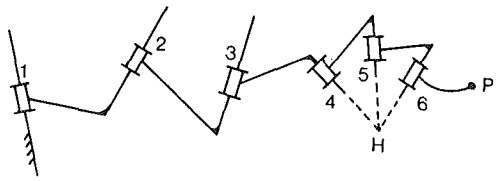

Fig. 7 A 6R manipulator in which the last three axes intersect orthogonally at a point H (i.e., $a_4 = a_5 = 0$, $\alpha_4 = 90$ deg, $\alpha_5 = 90$ deg)

is large whenever SHR (k) has a hole, or the axis $k-1$ passes through the void of SHR (k), or the axes k and $k-1$ are nearly the same whenever SHR (k) has a void.

With general manipulator configurations, the workspace $W_2(P)$ will in general have a hole as well as a void. In a general purpose manipulator, it is desirable to have the workspace $W_1(P)$ which is without any voids. The foregoing considerations then enable us to obtain the desired $W_1(P)$ solely from a proper relative positioning of axes 1 and 2.

It should be noted that the same $W_1(P)$ can be obtained with three axes as can be obtained with any greater number of axes. Insofar as $W_1(P)$ is concerned, there is no particular advantage in having more than three axes.

In general, the cross section of workspace $W_k(P)$ taken in, say, $x_k - z_k$ plane which contains axis k (Fig. 4), is obtained from the points of $W_{k+1}(P)$ by the following map: $(x_k, y_k, z_k) \rightarrow (\sqrt{x_k^2 + y_k^2}, 0, z_k)$.

Design Considerations

It is useful to divide the total workspace $W(P)$ into a primary[1] workspace $W^p(P)$ and a secondary workspace $W^s(P)$. In the primary workspace, each point is reachable from all directions, whereas in the secondary workspace the directions at each point are limited. In a general purpose manipulator, the objective is to maximize $W(P)$ and at the same time to have $W^p(P)$ as large a fraction of the total as possible.

It is known that any manipulator with three orthogonal revolute axes which intersect at one point P can have the property $W(P) = W^p(P)$ provided it is constructed so as to avoid mechanical interferences. Let us now discuss what happens to the workspace when P is not at the point of intersection of the three axes.

Consider the 6R manipulator with the last three axes intersecting orthogonally in point H as shown in Fig. 7. The point P is taken at a distance h from point H. For convenience, we will call distance h the "hand size." We now explore the influence of hand size on workspace.

If $h = 0$, i.e., point P coincides with H, the total workspace is primary workspace (since the position of H is not affected by the orientation of the last three links, and at each position of H every orientation of the last three links is possible). In this case, $W_1^p(P) = W_1(P) = W_1(H)$.

If $h \neq 0$, the total workspace of P is larger than that of H, while P's primary workspace is, in general, smaller. We have then $W_1^p(P) \subset W_1(H) \subset W_1(P)$. In other words, a nonzero hand size increases the total workspace, but decreases the primary workspace.

In order to determine whether a specific position P_i of point P belongs to the primary or secondary workspace, we introduce the linkage shown in Fig. 8. Here point P is replaced by a spherical joint fixed to ground at position P_i and the three orthogonally intersecting revolute joints are replaced by a spherical joint at point H. The linkage shown in Fig. 8 is kinematically equivalent to the original manipulator when point P is at position P_i. Hence the possible directions at which the manipulator can reach point P_i are the same as the allowable directions of the link HP_i in the 3R2S linkage of Fig. 8.

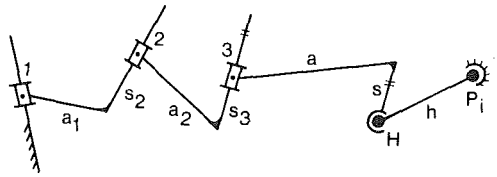

Fig. 8 A 3R2S linkage obtained by introducing spherical joints at H and P and by fixing point P at a point P_i in its workspace $W_1(P)$

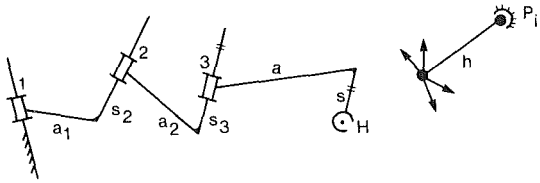

Fig. 9 The 3R2S does not exist if the point P_i is not contained in $W_1(P)$

It follows that all configurations of HP_i are possible only when the surface of the sphere of radius h and center at P_i lies entirely within the workspace of point H. In other words, point P_i lies in the primary workspace $W_1^p(P)$ if and only if the surface of the sphere of radius h and center at P_i lies completely within $W_1(H)$. If this is not the case, as in Fig. 9, P_i is not approachable from all directions or it does not belong to $W_1(P)$.

Figure 10 shows a cross section of $W_1(H)$ and the sections of spheres of radius h with different center points. We have then that P_k cannot lie in the primary workspace because part of the spherical surface is outside of the workspace boundary of $W_1(H)$. Since part of the spherical surface is inside $W_1(H)$, it does however belong to $W_1^s(P)$. Similarly, since the sphere centered at P_l crosses the internal void, we have $P_l \in W_1^s(P)$.

Since the spherical surface centered at P_j surrounds, but does not cross the internal void, it appears that P_j is a point of the primary workspace $W_1^p(P)$. However, if the internal void is a surface of revolution about axis 1, it must intersect the sphere even though it does not do so in the section shown, and so, in fact, in this case, P_j is a point of the secondary workspace $W_1^s(P)$. Clearly, P_i is a point of $W_1^p(P)$ since its sphere is entirely enclosed within $W_1(H)$, and P_m is not a point of $W_1(P)$ since its sphere has no points on $W_1(H)$.

It follows that if a sphere of radius h is moved so that its center lies on the boundary of $W_1(H)$, and if $W_1(H)$ has no internal voids, the outer envelope of the spheres is the

[1] Kumar and Waldron [4] use the term dextrous workspace for what we call primary workspace.

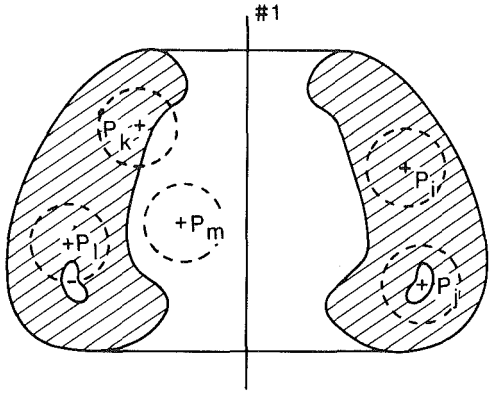

Fig. 10 The workspace $W_1(H)$, with voids, is shown in the section. Point P_l is in the primary workspace $W_1^p(P)$, points P_j, P_k, P_l lie in the secondary workspace $W_1^s(P)$, point P_m does not lie in the workspace $W_1(P)$.

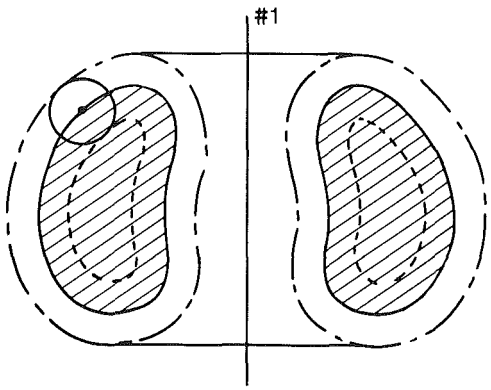

Fig. 11 Section of $W_1(H)$ is bounded by solid lines. The long and-short-dashed lines give the boundary of $W_1(P)$, while the short-dashed lines bound the subspace $W_1^p(P)$.

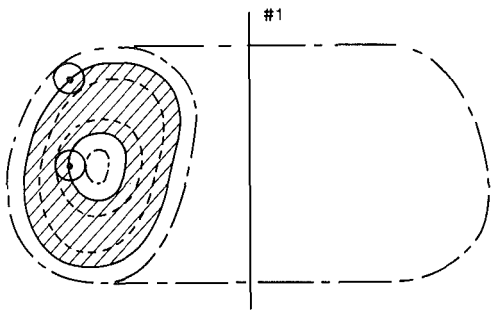

Fig. 12 Extension of case in Fig. 11 when $W_1(H)$ has a void and the hand size h is small compared to a typical cross-sectional dimension of the void

boundary of the total workspace W_1 (P) and the inside envelope as the boundary of the primary workspace W_1^p (P). Figure 11 illustrates this situation in a section of the workspace containing axis 1. If we have internal voids within W_1 (H), then the situation in the neighborhood of such boundaries is as shown in Fig. 12.

When h is large enough so that the W_1^p (P) region boundaries cross, then any point not in W_1^p (P) by virtue of its position relative to both the external boundary of W_1 (H) and the internal void boundary of W_1 (H) must be excluded from W_1^p (P). In general, when boundary curves cross each other, the more restrictive one takes precedence. In other words, a region of nonexisting workspace takes precedence over all others and a region of secondary workspace takes precedence over a region of primary workspace. So, for example, in Fig. 13, the region bounded by the short-dashed curve segments ADC and ABC (shown with double hatch marks) is the only

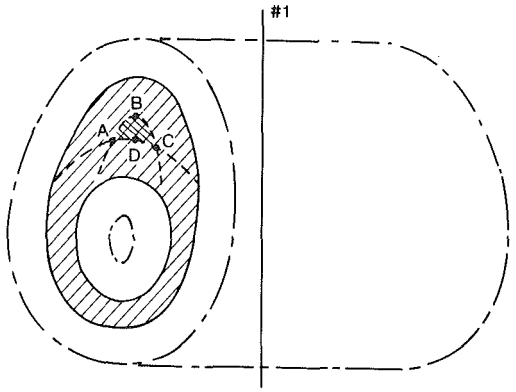

Fig. 13 Extension of case in Fig. 11 when $W_1(H)$ has a void and the hand size h is large compared to a typical cross-section dimension of the void. The small region ABCDA is $W_1^p(P)$.

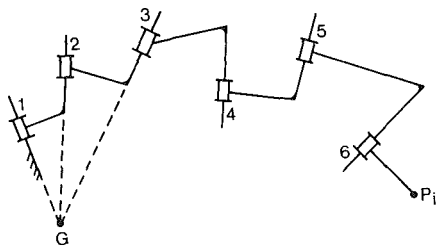

Fig. 14 A 6R manipulator with hand size h and the first three axes intersecting orthogonally at a common point G (i.e., $a_1 = a_2 = 0$, $\alpha_1 = 90$ deg, $\alpha_2 = 90$ deg)

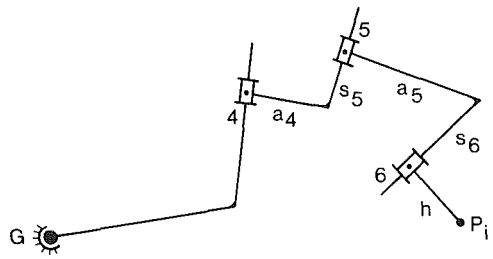

Fig. 15 A S3R manipulator which is kinematically equivalent to the 6R manipulator of Fig. 14

region with W_1^p (P) points in the section. The boundary of W_1 (P) remains the region between the two long and short-dashed curves.

For small hand sizes, a large fraction of the workspace W_1 (P) is primary workspace W_1^p (P). As the hand size increases, the primary workspace fraction decreases and eventually it vanishes. At the same time, the total workspace increases as h increases. When h exceeds a certain size, the workspace W_1 (P) undergoes a major structural change and no longer resembles that of W_1 (H).

From the point of view of design, it is not desirable to have voids in the primary workspace W_1^p (P) or the total workspace W_1 (P) of a general purpose manipulator. From the preceding discussion, it follows that if the workspace of point H, W_1 (H), has a void, then for $h \neq 0$ the primary workspace of point P, W_1^p (P), has a void even though the total workspace W_1 (P) may or may not have a void. Therefore the workspace W_1 (H) of point H should be free of voids.

First Three Axes Intersect

If, instead of the last three axes, we allow the first three axes to intersect orthogonally at a common point, we have the system shown in Fig. 14. This 6R manipulator is kinematically equivalent to the S3R manipulator shown in Fig. 15.

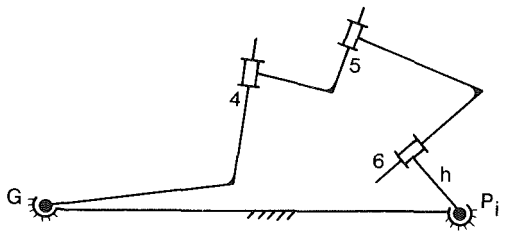

Fig. 16 The S3RS linkage obtained by introducing a spherical joint at P and by fixing point P at a point P_i in $W_1(P)$

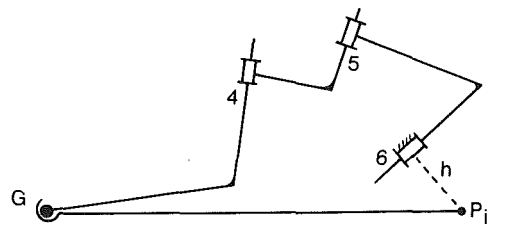

Fig. 17 The derived 3RS manipulator of "hand" size $\overline{GP_i}$. Figures 15 and 17 are related through kinematic inversion.

Since the entire system can rotate about point G, the workspace W_1 (P) is obviously a spherical shell. The radii of the shell are the maximum and minimum of distances $\overline{GP_i}$. If point P can reach point G, the workspace becomes a solid sphere (or a portion thereof if complete rotation about G is not possible).

In order to determine the primary workspace, we introduce a spherical joint at point P and connect this to the fixed side of the spherical joint at G. The result is a S3RS closed five-bar chain as shown in Fig. 16. Now it follows that if P_i is a point of the primary workspace, then the link of length h can take on every possible orientation with respect to the fixed link. However, the principle of kinematic inversion tells us that, at such a point, if we fixed link h and let the ground link (GP_i) move, it would be able to take on every possible orientation with respect to link h. But the inverted Fig. 16 is nothing other than the 3R2S of Fig. 8, where instead of h the size of the hand is now $\overline{GP_i}$.

It follows from this discussion that P_i of Figs. 14 and 15 will be a point of the primary workspace W_1^p (P) if and only if P_i is also a point of the primary workspace of the derived 3RS shown in Fig. 17. The conditions for P_i to be a point of the primary workspace of the system given in Fig. 17 are exactly the same as we have previously derived from Fig. 8. Hence it now immediately follows that, in Fig. 17.

(a) P_i must lie inside the workspace W_6 (G) of point G.

(b) A sphere of radius $\overline{GP_i}$ and center P_i must lie completely within the workspace W_6 (G).

Points P_i which meet both conditions (a) and (b) will belong to W_1^p (P). If the maximum value of $\overline{GP_i}$ for which both (a) and (b) are satisfied is R^*, it follows that the primary workspace of the original system, Figs. 14 and 15, is a solid sphere of radius R^* and center G.

From this we get three important design conclusions for 6R manipulators with the first three axes intersecting orthogonally in a common point G:

1 Point G must be inside W_1 (P), i.e., G must be a reachable point; otherwise there is no primary workspace W_1^p (P).

2 The workspace W_6 (G) of Fig. 17 should be a special SHR with no internal voids; this condition will usually result in a small R^*.

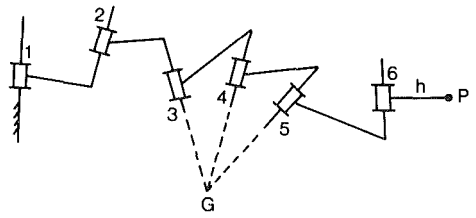

Fig. 18 A 6R manipulator with axes 3, 4, and 5 intersecting orthogonally (i.e., $a_3 = a_4 = 0$, $\alpha_3 = 90$ deg, $\alpha_4 = 90$ deg)

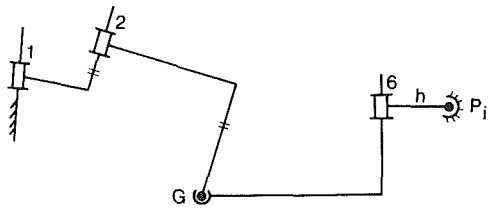

Fig. 19 The 2RSRS linkage obtained by introducing spherical joints at G and P, and fixing P at a point P_i in $W_1(P)$

3 Even though h does not appear explicitly in the foregoing criteria, it markedly affects the position of P_i and hence strongly influences the value of R^*.

Manipulators With Other Joints and More Than 6 Degrees of Freedom

The arguments and results developed herein are valid for systems with any number of degrees of freedom. For less than 6 degrees of freedom, the conditions for W_1^p (P) will generally not be satisfied. For systems with more than 6 freedoms, the conditions can generally be satisfied more easily than with a 6-degree-of-freedom system. The nature of the workspace of any system with the last three revolute axes intersecting orthogonally is exactly the same as determined for the configuration of Fig. 7, and the nature of any system with its first three axes mutually intersecting orthogonal revolutes is exactly as for Fig. 14. This holds for any chains of the form N-$\overline{3R}$ and $\overline{3R}$-N, where $\overline{3R}$ represents three mutually intersecting orthogonal revolute axes and N is any system of links and joints.

Hence our analysis holds for chains with prismatic joints, for example, and for systems with 7 and 8 degrees of freedom. When prismatic joints are present, they can be assumed to have reasonably finite joint travel. If a manipulator has an RP-N structure, then its workspace has no voids. With a PR-N structure, the workspace has no voids if the axes (direction) of the P joint and the second R joint are at nearly 90 deg; otherwise, the workspace may have voids. The precise range of angle, between the P and R joint axes, to eliminate the void in the workspace depends upon the size of the hole in SHR (2).

Although we have addressed ourselves to 6-degree-of-freedom revolute chains, the only real restriction on the results dealing with hand size is that we start or end with a $\overline{3R}$ configuration.

Intermediate Axes Intersect

We now consider the two remaining cases of three intersecting axes: If axes 3, 4, and 5 intersect orthogonally, as shown in Fig. 18, the manipulator is kinematically equivalent to a 2RSR chain. The workspace of point G with respect to axis 1, i.e., W_1 (G), is obviously a torus. The workspace of point P about axis 3 is a spherical shell with center at G and inner radius $\bar{R}$ = min (GP) and outer radius R^* = max (GP). By tracing the reach of point P with respect to G at each point on the torus W_1 (G), we obtain the SHR (1) which

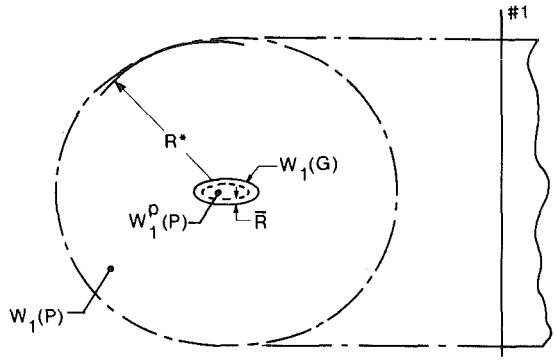

Fig. 20 Interiors of short-dashed and long-short-dashed boundaries are sections of $W_1^p(P)$ and $W_1(P)$, respectively, for manipulator in Fig. 18. Solid curve represents $W_1(G)$.

represents the workspace W_1 (P). If $\bar{R}$ is sufficiently small compared to a typical cross-sectional dimension of the void of torus W_1 (G), then the size and shape of W_1 (P) is independent of $\bar{R}$. In addition, if R^* is slightly larger than $\bar{R}$, W_1 (P) is a SHR with a void. Its wall thickness is $2R^*$. When R^* is much greater than a typical cross-sectional dimension of the void of torus W_1 (G), the workspace W_1 (P) becomes a special SHR without a void. This situation is shown in Fig. 20 where the cross section of W_1 (P) is the interior of the boundary with long and short dashes.

In order to determine if a point P_i belongs to the primary workspace W_1^p (P), we introduce a fixed spherical joint at P_i as shown in Fig. 19. If P_i is a point of W_1^p (P), then the hand h can be placed in any position about P_i. Clearly, the hand can spin about the line $\overline{P_iG}$. For the point P_i to be in the primary workspace, the linkage in Fig. 19 should exist for all orientations of the line $\overline{GP_i}$ about the point P_i. We note that W_1 (G) is a torus, while G relative to P_i gives a spherical shell centered at P_i with inner and outer radii $\bar{R}$ and R^*, respectively. If P_i is so located that the inner surface of the shell lies completely within the torus W_1 (G), and the outer surface of the shell is large enough so that the shell contains a portion of W_1 (G) which is pierced by the radial rays emanating from P_i, then P_i lies in the primary workspace W_1^p (P). The first condition leads to short dashed boundary of W_1^p (P) in Fig. 20. The second condition is satisfied because R^* is large compared to the void in W_1 (G). As a result, W_1^p (P) is the interior of the short dashed boundary in Fig. 20. When $\bar{R}$ and R^* do not satisfy the aforementioned conditions, then W_1 (P) is a general SHR and W_1^p (P) is much more difficult to determine.

The fourth (and final) possible combination of three intersecting orthogonal axes occurs when axes 2, 3, and 4 are orthogonal and mutually intersecting. This manipulator is kinematically equivalent to the RS2R manipulator shown in Fig. 21.

The condition for P to be a point of W_1^p (P) follows easily from the figure. If we fix link h in a given position, then breaking the linkage at point G yields that W_6 (G) is a torus while W_1 (G) is of course a circle. For P_i to be a point of W_1^p (P), we must be able to rotate the torus W_6 (G) about P_i (as spherical center) and have the circle W_1 (G) intersect the torus at each position. This is only possible if the torus has special positions relative to P_i and the circle. For example, if P_i is close to or at the center of the torus, and the torus has a nearly spherical shape, then P_i will be part of the primary workspace. On the other hand, if P_i is outside the circle and at any distance from the torus' axis, it will not belong to the primary workspace.

The conclusion is that as h increases, the primary workspace decreases. For maximum primary workspace, h must be kept small and the torus must approach a spherical as opposed to a donut shape.

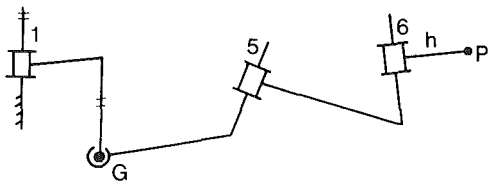

Fig. 21 The equivalent RS2R manipulator when axes 2, 3, and 4 of a 6R manipulator are mutually orthogonal and intersect in a point G (i.e., $a_2 = a_3 = 0$, $\alpha_2 = 90$ deg, $\alpha_3 = 90$ deg)

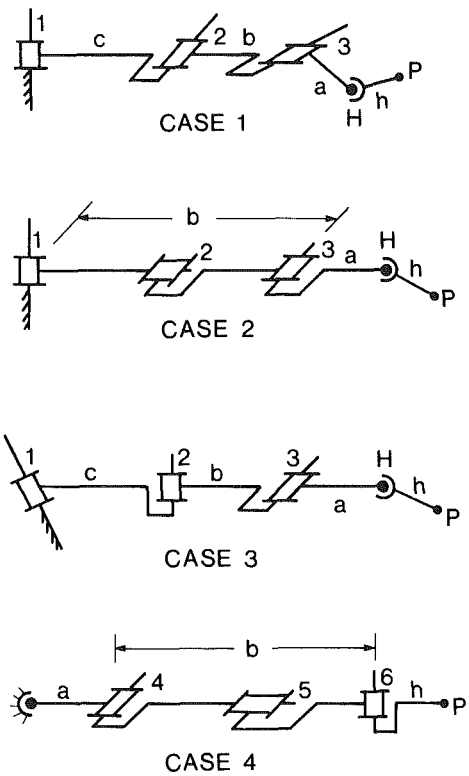

Fig. 22 Manipulator configurations considered in illustrative examples

The total workspace of P is a general SHR obtained by tracing the reach of point P with respect to G ($\bar{R} \leq GP \leq R^*$) at each point of the circle W_1 (G) or, equivalently, by revolving the hollow spherical shell with center at G and radii $\bar{R}$ and R^* about the axis 1. Thus W_1 (P) is a right circular toroidal space except when the axis 1 passes through the void of the shell.

Examples

The new concepts presented in the paper are now illustrated by means of four manipulator configurations shown in Fig. 22.

Manipulator Case 1. Let $s_1 = s_2 = s = 0$, $\alpha_1 = 90$ deg, α_2 arbitrary, $a_1 = c$, $a_2 = b$, $a \leq b \leq c$ in Figs. 7 and 8. The workspace W_3 (H) is circle (3), W_2 (H) is torus (2), and W_1 (H) is SHR (1). The workspace W_1 (H) is shown in Fig. 23(*a*). It has an internal void if $a \neq b$. The volume of W_1 (H) is $8\pi^2$ abc. The shape and volume of W_1 (H) are not influenced by the value of the angle α_2. The primary and secondary workspaces W_1^p (P) and W_1 (P) of the terminal point P when the hand size is $h \neq 0$ can be obtained as shown

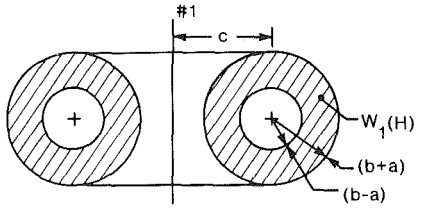

Fig. 23(*a*) The workspace $W_1(H)$ for manipulator case 1

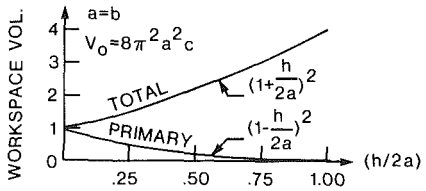

Fig. 23(*b*) Volumes of primary $W_1^p(P)$ and total $W_1(P)$ in relation to the hand size h when $W_1(H)$ has no void

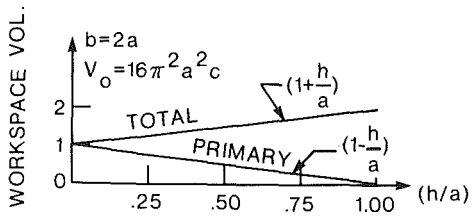

Fig. 23(*c*) Volumes of $W_1^p(P)$ and $W_1(P)$ in relation to the hand size h when $W_1(H)$ has a void

in Figs. 11 and 12. The volumes of workspaces W_1^p (P) and W_1 (P) are plotted with respect to hand size in Fig. 23(*b*) for the case $a = b$ (no void in W_1 (H)) in the range $0 \le h \le 2a$. A similar plot when $b = 2a$ is shown in Fig 23(*c*). Both plots have been normalized with respect to the workspace volume when $h = 0$ (i.e., the volume of W_1 (H)).

Manipulator Case 2. Let $s_1 = s = 0$, $s_2 = b$, $\alpha_1 = \alpha_2 = 90$ deg, $a_1 = a_2 = 0$, $a \le b$ in Figs. 7 and 8. The workspace W_3 (H) is circle (3), W_2 (H) is sphere (2) and W_1 (H) is a right circular toroidal space SHR (1). The workspace W_1 (H) is free of voids and its volume is $2\pi^2a^2b$. In the construction of this manipulator, the second revolute joint can be placed anywhere on the shortest distance line for axes 1 and 3, so long as the distance between these two axes is b. The plots of the volumes of the primary and secondary workspaces W_1^p (P) and W_1 (P) of the terminal point P with respect to hand size h are identical to the ones in Fig. 23(*b*) except that "$2a$" is replaced by "a".

Manipulator Case 3. Let $s_1 = s_2 = s = 0$, α_1 arbitrary, $\alpha_2 = 90$ deg, $a_1 = c$, $a_2 = b$. The workspace W_3 (H) is circle (3) and W_2 (H) is torus (2). The shape of W_1 (H) depends upon the angle α_1 and the relative magnitudes of a and b. If $a \ge b$, then W_1 (H) is a SHR without any void. If $a < b$ and $\alpha_1 = 90$ deg, we obtain the workspace shown in Fig. 23(*a*); it has a void. As the angle α_1 is reduced, still keeping $a < b$, the size of the void is reduced and the shape of W_1 (H) is a general SHR (3). If $\alpha_1 <$ arc sin (a/b), then the void in W_1 (H) is eliminated. The nature of W_1 (H) when $\alpha_1 = 0$ is shown in Fig. 24(*a*). Its volume is $(8\pi abc + 2\pi^2a^2c)$. Figure 24(*b*) shows the volumes of primary W_1^p (P) and total W_1 (P) when $b = \pi a/2$. If, in the manipulator Case 2 (Fig. 22), the second joint is replaced by a prismatic joint of travel $2b$ such that the maximum and minimum distances between axes 1 and 3 are $c+b$ and $c-b$, respectively, then this RPRS manipulator also has the workspace W_1 (H) shown in Fig. 24(*a*), and Fig. 24(*b*) is applicable as well.

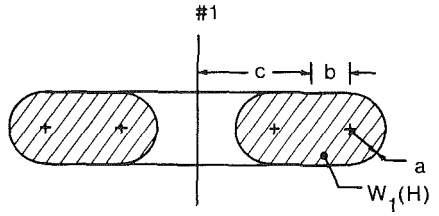

Fig. 24(*a*) Workspace $W_1(H)$ for manipulator case 3 when axes 1 and 2 are parallel

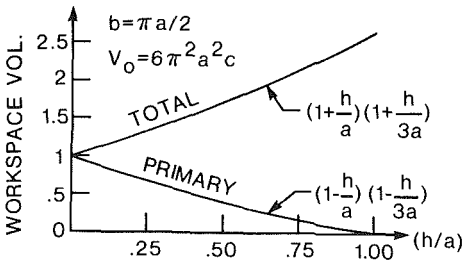

Fig. 24(*b*) Volumes of primary $W_1^p(P)$ and total $W_1(P)$ with respect to hand size h

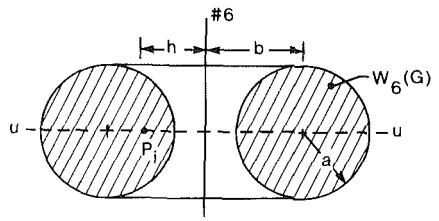

Fig. 25(*a*) Workspace $W_6(G)$ of the derived 3RS manipulator from manipulator case 4

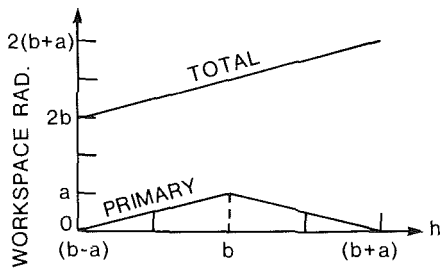

Fig. 25(*b*) Radii of the primary $W_1^p(P)$ and total $W_1(P)$ of the original S3R manipulator as shown with respect to hand size h

Manipulator Case 4. Let $s_G = s_6 = 0$, $s_5 = b$, $\alpha_4 = \alpha_5 = 90$ deg, $a_G = a$, $a_4 = a_5 = 0$, $a \le b$ in Fig. 15. This manipulator is related to Case 2 which we have considered through the inversion shown in Fig. 17. The workspace W_6 (G) of the inverted manipulator is as shown in Fig. 25(*a*). The point P_i lies on the line $u-u$. R^* is defined as the radius of the largest sphere within the workspace W_6 (G) that can be drawn with P_i as center. Therefore, $b-a \le h \le a+b$ and R^* = min. $(h-b+a, b+a-h)$. It then follows that the radius of the primary workspace W_1^p (P) of the original manipulator (Fig. 15 with specified dimensions) is a sphere of radius R^* = min. $(h-b+a, b+a-h)$ whenever $b-a \le h \le b+a$. It should be noted that this manipulator has no primary workspace if the hand is either too small $(h < b-a)$ or too large $(h > b+a)$.

The total workspace of this manipulator is a sphere of radius $(a+b+h)$, assuming that $b-a \le h \le b+a$. The radii of the primary and total workspace of point P with respect to hand size h are shown in Fig. 25(*b*) in the appropriate range of

h. For any given a and b such that $a \leq b$, the primary workspace is largest when $h = b$.

Conclusions

We have shown that it is possible to analyze the shape of workspaces and determine the influence of hand size on the ratio of primary to total workspace. We have treated the cases of three mutually orthogonal intersecting axes in detail and provided a basis for designers to rationally determine the dimensions of 6-degree-of-freedom manipulators. These results can be applied to designing for a total workspace or for a certain primary workspace; most important, they deal with the much neglected question of hand size.

Acknowledgments

The financial support of the National Science Foundation under grant ENG 79-23193 to the University of Illinois at Chicago Circle and grant ENG 79-10313 to Stanford University is acknowledged.

References

1 Roth, B., "Performance Evaluation of Manipulators from a Kinematic Viewpoint," NBS Special Publication *Performance Evaluation of Programmable Robots and Manipulators*, 1975, pp. 39–61.

2 Roth, B., "Robots," *Applied Mechanics Reviews*, Vol. 31, No. 11, 1978, pp. 1511–1519.

3 Kumar, A., and Waldron, K. J., "The Dextrous Workspace," ASME Paper No. 80-DET-108, 1980.

4 Kumar, A., and Waldron, K. J., "The Workspace of a Mechanical Manipulator," ASME JOURNAL OF MECHANICAL DESIGN, Vol. 103, No. 3, July 1981, pp. 665–672.

5 Vertut, J., "Contribution to Analyze Manipulator Morphology Coverage and Dexterity," *On the Theory and Practice of Manipulators*, Vol. 1, Springer-Verlag, 1974, pp. 277–289.

6 Fichter, E. F., and Hunt, K. H., "The Fecund Torus, Its Bitangent Circles and Derived Linkages," *Mechanism and Machine Theory*, Vol. 10, 1975, pp. 167–176.